Sr Lattice Clock at 1 x 10 16 Fractional Uncertainty by Remote Optical Evaluation with a Ca Clock

A. D. Ludlow, *et al.*

Science **319**, 1805 (2008);
DOI: 10.1126/science.1153341

Science (print ISSN 0036-8075; online ISSN 1095-9203) is published weekly, except the last week in December, by the American Association for the Advancement of Science, 1200 New York Avenue NW, Washington, DC 20005.

15. F. P. Gavriil, V. M. Kaspi, *Astrophys. J.* **609**, L67 (2004).
16. P. M. Woods *et al.*, *Astrophys. J.* **605**, 378 (2004).
17. R. Dib, V. M. Kaspi, F. P. Gavriil, *Astrophys. J.* **666**, 1152 (2007).
18. C. R. Tam *et al.*, http://arxiv.org/abs/0712.2856.
19. E. Göğüs *et al.*, *Astrophys. J.* **558**, 228 (2001).
20. C. Thompson, M. Lyutikov, S. R. Kulkarni, *Astrophys. J.* **574**, 332 (2002).
21. A. M. Beloborodov, C. Thompson, *Astrophys. J.* **657**, 967 (2007).
22. C. Thompson, R. C. Duncan, *Astrophys. J.* **408**, 194 (1993).
23. L. Ferrario, D. Wickramasinghe, *Mon. Not. R. Astron. Soc.* **367**, 1323 (2006).
24. D. Bhattacharya, V. Soni, http://arxiv.org/abs/0705.0592.
25. A. G. Lyne, in *Young Neutron Stars and Their Environments, IAU Symposium 218*, F. Camilo, B. M. Gaensler, Eds. (Astronomical Society of the Pacific, San Francisco, 2004), pp. 257–260.
26. A. K. Harding, I. Contopoulos, D. Kazanas, *Astrophys. J.* **525**, L125 (1999).
27. M. E. Gonzalez, V. M. Kaspi, F. Camilo, B. M. Gaensler, M. J. Pivovaroff, *Astrophys. J.* **630**, 489 (2005).
28. F. Camilo *et al.*, *Nature* **442**, 892 (2006).
29. F. Camilo, S. M. Ransom, J. P. Halpern, J. Reynolds, *Astrophys. J.* **666**, L93 (2007).
30. K. Hurley *et al.*, *Nature* **434**, 1098 (2005).
31. D. J. Helfand, B. F. Collins, E. V. Gotthelf, *Astrophys. J.* **582**, 783 (2003).
32. C. Y. Ng, P. O. Slane, B. M. Gaensler, J. P. Hughes, 10th Meeting of the High Energy Astrophysics Division of the American Astronomical Society, Los Angeles, CA, 2008.
33. H. S. Kumar, S. Safi-Harb, http://arxiv.org/abs/0802.1242.
34. We thank T. Strohmayer for assistance and A. Harding and D. Kazanas for discussion. M.A.L. is a Natural Sciences and Engineering Research Council (NSERC) PGS-D fellow. Support for this work was also provided by an NSERC Discovery Grant Rgpin 228738-03, an R. Howard Webster Fellowship of the Canadian Institute for Advanced Research, Les Fonds de la Recherche sur la Nature et les Technologies, a Canada Research Chair and the Lorne Trottier Chair in Astrophysics and Cosmology to V.M.K., and RXTE grants NNG05GM87G and N5-RXTE05-34 to E.V.G. This research made use of data obtained through the High Energy Astrophysics Science Archive Research Center Online Service, provided by the NASA/Goddard Space Flight Center.

Supporting Online Material
www.sciencemag.org/cgi/content/full/1153465/DC1
SOM Text

27 November 2007; accepted 13 February 2008
Published online 21 February 2008;
10.1126/science.1153465
Include this information when citing this paper.

Sr Lattice Clock at 1×10^{-16} Fractional Uncertainty by Remote Optical Evaluation with a Ca Clock

A. D. Ludlow,[1] T. Zelevinsky,[1]* G. K. Campbell,[1] S. Blatt,[1] M. M. Boyd,[1] M. H. G. de Miranda,[1] M. J. Martin,[1] J. W. Thomsen,[1]† S. M. Foreman,[1]‡ Jun Ye,[1]§ T. M. Fortier,[2] J. E. Stalnaker,[2]‖ S. A. Diddams,[2] Y. Le Coq,[2] Z. W. Barber,[2] N. Poli,[2]¶ N. D. Lemke,[2] K. M. Beck,[2] C. W. Oates[2]

Optical atomic clocks promise timekeeping at the highest precision and accuracy, owing to their high operating frequencies. Rigorous evaluations of these clocks require direct comparisons between them. We have realized a high-performance remote comparison of optical clocks over kilometer-scale urban distances, a key step for development, dissemination, and application of these optical standards. Through this remote comparison and a proper design of lattice-confined neutral atoms for clock operation, we evaluate the uncertainty of a strontium (Sr) optical lattice clock at the 1×10^{-16} fractional level, surpassing the current best evaluations of cesium (Cs) primary standards. We also report on the observation of density-dependent effects in the spin-polarized fermionic sample and discuss the current limiting effect of blackbody radiation–induced frequency shifts.

The quest to develop more accurate quantum frequency standards has produced a detailed understanding of matter-field interactions and a vast toolbox of techniques for precision measurement and quantum state control. Historically, the neutral ^{133}Cs microwave clock transition has offered the highest realizable accuracy for state-of-the-art frequency standards (*1*, *2*). In recent years, interest in and performance of standards based on optical atomic transitions have grown (*3*), driven by their superior resonance quality factors (*4*). The most accurate optical clocks are presently based on single trapped ions (*5*), due to the exquisite control possible over their electronic and motional quantum states, as demonstrated in both clock and quantum information experiments (e.g., *5*–*8*). Although neutral atoms (e.g., *9*–*12*) enjoy high measurement precision from the use of large ensembles, a longstanding challenge for these optically based systems is achieving control and measurement at similar uncertainties as for single trapped particles. We report here a systematic uncertainty evaluation for a neutral Sr optical atomic standard at the 10^{-16} fractional level, surpassing the best evaluations of Cs fountain primary standards. This demonstrates control of clock states for large ensembles of atoms approaching that of the best single ion systems. Precise understanding of interactions among lattice-confined atoms will allow clean preparation, control, and readout of atoms for quantum simulations (*13*). Our measurements with thousands of atoms approach the fundamental quantum noise limit, opening the possibility of spin squeezing in optical lattices to combine precision measurement and quantum optics.

Rigorous determination of clock performance can only be achieved by comparing different clocks of similar performance. Although Cs primary standards have served as the best-characterized clock references, direct comparison between optical atomic clocks has now become essential as the uncertainties in the realized, unperturbed clock frequencies are now smaller than those for the best Cs primary standards [as demonstrated in this work and the single ion clock (*5*)]. These systematic uncertainties form the essential element of clock accuracy. Unfortunately, the current complexity of these high-performing optical clocks limits the availability of multiple systems in a single laboratory. Comparing remotely located clocks can circumvent this difficulty. However, traditional methods for these remote clock comparisons such as global positioning satellite links or microwave frequency networks are increasingly inadequate for transferring optical clock signals due to their insufficient stability. All-optical comparison between remote optical clocks permits measurement without compromising the clocks' high precision and ultimately will facilitate tests of fundamental physical laws (*14*) and enable long baseline gravitational measurements (*15*) or long-distance quantum entanglement networks. The optical comparison between the JILA Sr lattice clock on the University of Colorado campus and the calcium (Ca) optical clock at the National Institute of Standards and Technology (NIST) Boulder laboratories is accomplished remotely by a 4-km optical fiber link.

The optical link uses coherent optical carrier transfer [Fig. 1, with more technical details provided in (*16*)]. A self-referenced octave-spanning optical frequency comb at JILA is phase-locked to the Sr clock laser operating at 698 nm. A continuous wave Nd:yttrium-aluminum-garnet (cw Nd:YAG) laser at 1064 nm is phase-locked to the same frequency comb, and its light is transferred to NIST by a phase-noise-cancelled fiber link. In this way, the Sr timekeeping is phase-coherently

[1]JILA, National Institute of Standards and Technology, and University of Colorado, Department of Physics, University of Colorado, Boulder, CO 80309–0440, USA. [2]National Institute of Standards and Technology, 325 Broadway, Boulder, CO 80305, USA.

*Present address: Columbia University, New York, NY 10027, USA.
†Permanent address: Niels Bohr Institute, Copenhagen, Denmark.
‡Present address: Stanford University, Palo Alto, CA 94305, USA.
‖Present address: Oberlin College, Oberlin, OH 44074, USA.
¶Permanent address: Università di Firenze, Italy.
§To whom correspondence should be addressed. E-mail: ye@jila.colorado.edu

transmitted to NIST with a measured transfer instability of $6 \times 10^{-18}/\sqrt{\tau}$ (*17*), where τ is the averaging time. A 10^{-15} fraction of the Sr clock frequency is 0.4 Hz. The transferred Nd:YAG laser light is then frequency-counted against another octave-spanning optical frequency comb at NIST (*18*), which is phase-stabilized to the Ca optical clock operating at 657 nm (*19*). Both comb systems have demonstrated the capability of supporting optical clocks at below the 10^{-18} level (*16*).

For Sr clock operation, ~4000 ^{87}Sr (nuclear spin $I = 9/2$) atoms are laser cooled to 2.5 μK and confined in a one-dimensional (1D) optical lattice. Spectroscopic probing of the $^1S_0$-$^3P_0$ clock transition (Fig. 2A) is performed along the strong confinement axis of the lattice, in the Lamb-Dicke regime and the resolved sideband limit (*8*). Clock interrogation is thus highly immune to Doppler and recoil effects. Using optical pumping, the atoms are (doubly) spin-polarized and occupy only the two states $m_F = \pm 9/2$ (m_F = magnetic quantum number). Figure 2B shows spectra of the π clock transitions ($\Delta m_F = 0$) with and without the optical pumping. With the spin-polarized sample under a bias magnetic field, we interrogate the isolated $m_F = \pm 9/2$ clock transitions for 80 ms, allowing Fourier-limited spectral linewidths of 10 Hz. For these conditions, quantum projection noise would limit the Sr clock stability to $7 \times 10^{-16}/\sqrt{\tau}$ (*20*). To characterize the potential signal-to-noise ratio of the present system, we excite atoms on resonance using a short, strong Rabi pulse to power and Fourier-broaden the excitation, reducing the effect of laser frequency noise. We then measure the normalized, shot-to-shot excitation fraction as we reload the optical lattice with new samples. The excitation fluctuations are consistent with the expected quantum projection noise. However, during clock operation, the probe laser frequency noise deteriorates clock stability. High-frequency laser noise is aliased into the low-frequency measurement band because of the optical Dick effect (*21*). This effect is exacerbated by dead time (1 s) between measurements, which includes cooling the atoms, loading the lattice, polarizing the atomic sample, and determining the populations. The measured frequency noise spectrum of our probing laser (*22*) limits clock stability to $2 \times 10^{-15}/\sqrt{\tau}$.

Figure 2C summarizes these different stability figures for the Sr lattice clock, including the measured Allan deviation between the Sr clock at JILA and the Ca clock at NIST. The Ca clock is a simple and robust system that uses freely expanding cold atoms. Like a hydrogen maser, it serves as a highly stable frequency reference, but with 100 times better stability at short times. Indeed, the stability of the Sr-Ca comparison can reach below 3×10^{-16} after 200 s. However, the Ca clock is susceptible to long-term (>1000 s) drifts due to residual Doppler effects. To optimize evaluation of the Sr clock uncertainties, frequency measurements are thus made in 100-s time windows. To remove sensitivity to long-term Ca drifts, these 100-s windows are interleaved as a particular parameter of the Sr clock is systematically varied. Typically, the parameter is toggled between two settings for two consecutive 100-s windows, and a Sr clock frequency shift is measured between them. Many such pairs are accumulated to average to a measurement precision below 1×10^{-16}, enabling rigorous evaluations of key Sr clock frequency shifts at this level. This measurement approach is facilitated by the robustness of these optical clocks, because both systems are regularly operated on-demand for time scales of a day.

Optical confinement of the Sr atoms occurs at a "magic" wavelength where the polarizabilities of the two clock states are equal (*23*–*25*). The dipole polarizability can be expanded into the scalar, vector, and tensor terms with zero, linear, and quadratic dependence on the m_F of the clock state, respectively (*26*). The opposite symmetries of the vector and tensor polarizabilities facilitate orthogonalization of their effects experimentally. Because of the antisymmetric m_F-dependence of the vector polarizability, clock stabilization to the average of the ±9/2 transitions eliminates dependence of the clock frequency on the vector light shift. This effect would instead be observed as a change in the frequency separation between the two ±9/2 transitions added to the Zeeman splitting from the bias magnetic field. The averaged clock transition retains dependence on the symmetric tensor polarizabilty, which simply adds a $|m_F|$-dependent offset to the dominant scalar term. Thus, for a given lattice polarization, each spin state has a well-defined magic wavelength for insensitive confinement. The lattice laser providing the atomic confinement is frequency stabilized to the optical frequency comb, which itself is locked to the Sr clock laser. At a lattice peak intensity of $I_0 = 3$ kW/cm^2 and at the typical operating laser frequency, we observe a $6.5(5) \times 10^{-16}$ shift in the clock frequency compared to zero intensity (see Fig. 3A). Combined with our previous measurement of the weak clock sensitivity to the lattice frequency (*24*), we extrapolate the magic lattice frequency to be 368,554.68(18) GHz, in agreement with previous measurements (*9*, *23*–*25*). Although tensor shifts are estimated to be small,

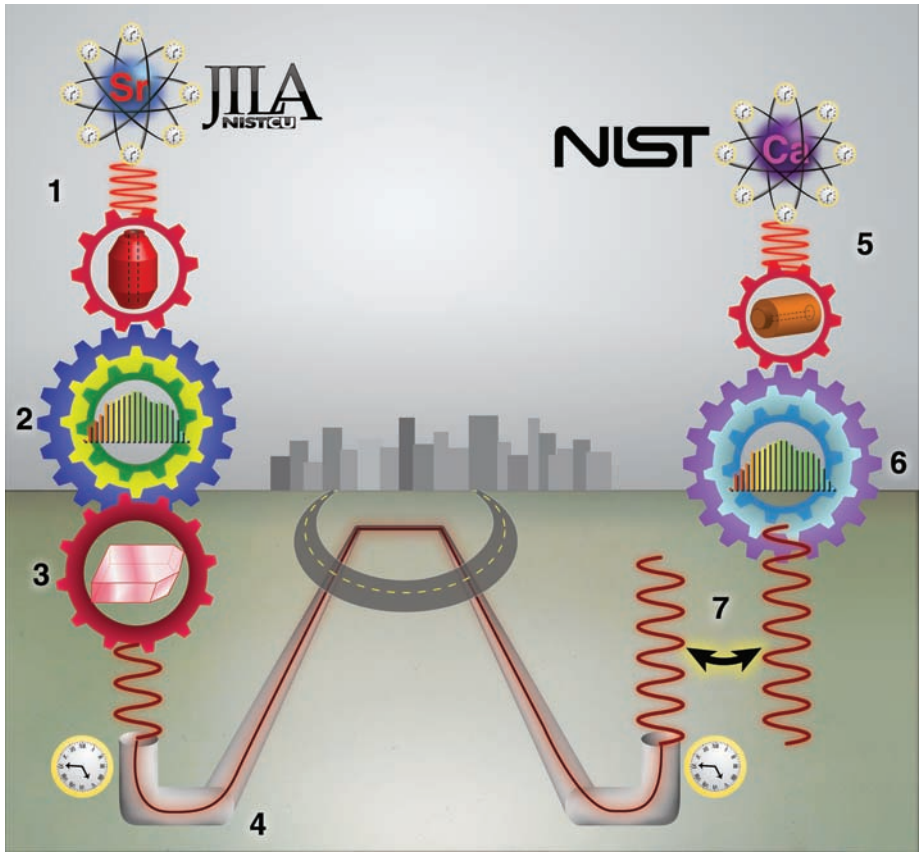

Fig. 1. Remote optical clock comparison. The atomic reference is counted and distributed in direct analogy to traditional clocks using mechanical gears, albeit at optical frequencies. The Sr atomic clock at JILA [1, lattice trapped Sr system and a laser at 698 nm stabilized to vertically mounted high-finesse optical cavity (*22*)] serves as the atomic standard to which an optical frequency comb (2) is phase-locked. A cw Nd:YAG laser at 1064 nm (3, a nonplanar ring oscillator) is phase-locked to the same frequency comb and transferred to NIST by a phase-noise–cancelled fiber link (4). The 1064 light emerges from the fiber at NIST and is phase coherent with the light originating from JILA, as symbolized by the synchronized clocks on either fiber end. The Ca optical clock at NIST (5, free space Ca atoms and a laser stabilized to a horizontally mounted optical cavity operating at 657 nm) is the atomic reference to which an optical frequency comb (6) at NIST is phase-locked. The clock comparison (7) is made by a heterodyne measurement between the NIST frequency comb and the 1064-nm transmitted light.

we clarify that this magic frequency is specified for the π-transitions from the ±9/2 nuclear spin states. The hyperpolarizability effect (fourth order in electric field) has been measured (*25*) and for our operating conditions is $2(2) \times 10^{-17}$.

As with the lattice vector Stark shift, the first-order Zeeman shift is cancelled because of the antisymmetric linear dependence of the ±9/2 states on the magnetic field. To individually address spin states, we choose a bias field (B_0 = 20 μT) large enough to resolve π transitions and reduce line pulling from residual populations of other spin states but small enough to keep the spin-symmetric second-order Zeeman shift small. The size of B is calibrated by measuring the frequency spacing between two spin-state transitions (*26*). To determine the second-order sensitivity and the first-order insensitivity, we measure clock frequency shifts as a function of B. An example of one such measurement is shown in Fig. 3C. Each set of data is fit to a second-order polynomial. The fit parameters of many such sets of data are averaged, and the first-order shift is found to be $2(2) \times 10^{-17}$ (for B_0), consistent with zero. The second-order shift is $2.3(2) \times 10^{-17}$, and the measured shift coefficient is $5.8(8) \times 10^{-8}$ T^{-2}, consistent with other measurements (*12*).

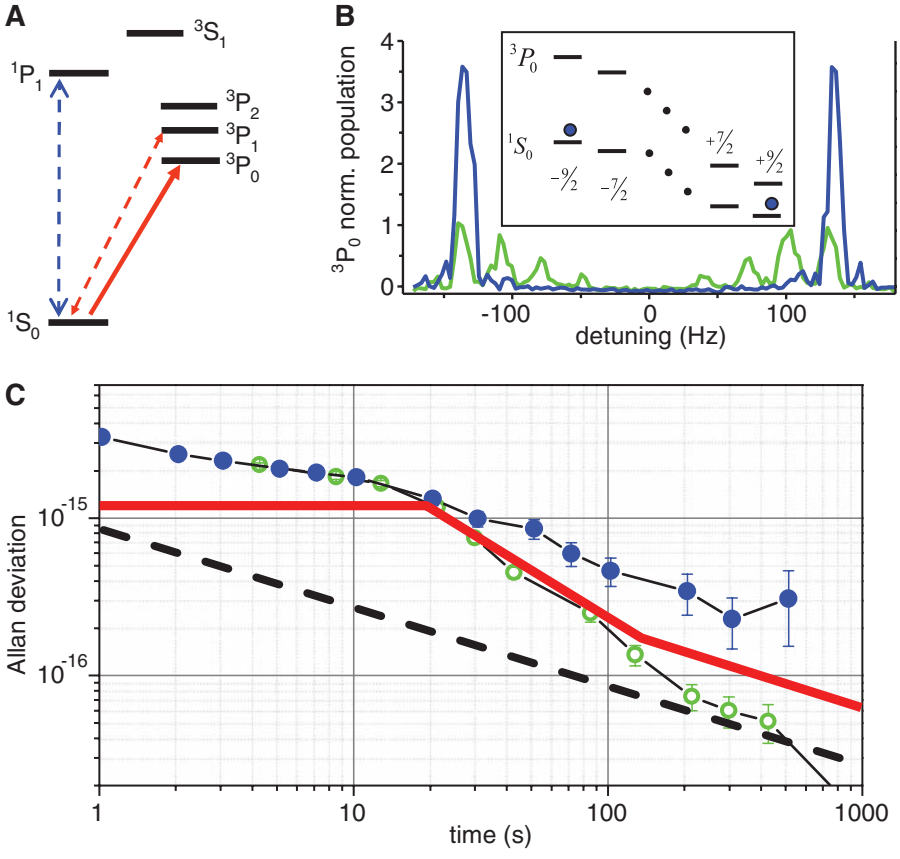

Fig. 2. Sr clock operation. (**A**) Sr energy level diagram. The red and blue dashed lines indicate laser cooling transitions and the solid red line the clock transition. (**B**) Spectroscopic probing of the clock transition under a bias magnetic field to lift the nuclear spin state degeneracy. π transitions with (without) spin polarization optical pumping are shown in blue (green), normalized to the unpolarized ±9/2 peaks. The inset indicates the individual nuclear spin states. After spin polarization, the population resides only in the $m_F = \pm 9/2$ $^1S_0$ states. (**C**) Stability figures for the Sr optical clock as a function of averaging time. Black dashed line: quantum projection noise limit. Blue filled circles: Sr-Ca remote comparison. Green open circles: in-loop stability, based on the error signal of the atom-laser servo. Red solid line: calculated stability, consisting of the free running laser stability (*22*) at short time scales, atom-laser servo operation at intermediate time scales, and the Dick effect limit at long time scales.

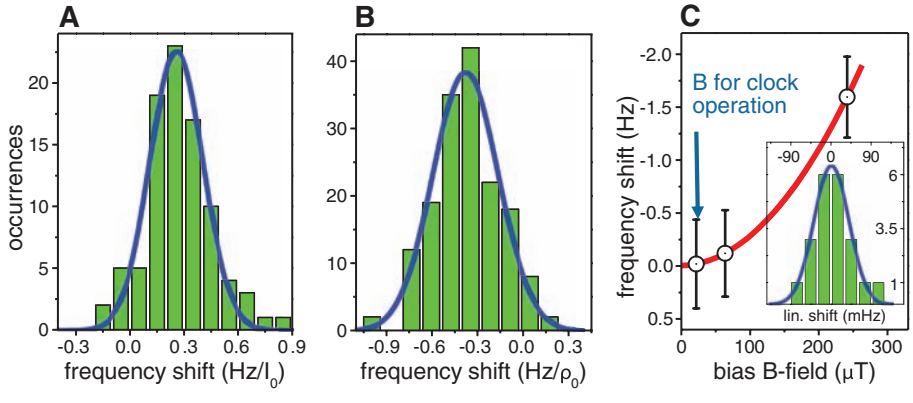

Fig. 3. Clock shift sensitivities. Histogram of clock shift sensitivity to (**A**) the lattice laser intensity slightly away from the magic frequency and (**B**) the atomic density. (**C**) One of 20 data sets indicating the clock sensitivity to magnetic fields. The inset to (C) shows the histogram of the linear Zeeman shift evaluated at B_0, based on the 20 data sets.

Although an ensemble of neutral atoms enables large signal-to-noise measurements for high precision and stability, interactions among colliding atoms can result in frequency shifts that degrade the system accuracy. For the case of lattice clocks, unity (or less)–filled sites in a 3D lattice can keep atomic spacing to at least half an optical wavelength and thus reduce interatomic interactions (*23*, *27*). For the 1D lattice, use of identical ^{87}Sr fermions at ultracold temperature can exploit the Pauli exclusion principle to reduce interactions (*28*) by eliminating even-wave collisions. Ground-state ($^1S_0$-$^1S_0$) and excited-state ($^3P_0$-$^3P_0$) interatomic potentials have been theoretically calculated (*29*), but the only experimental measurements exist in photoassociation spectroscopy of even isotopes of Sr (*30*). We have observed a density-dependent frequency shift even when the atoms are polarized to a single spin state, indicating possible P-wave interactions or the loss of indistinguishability due to inhomogeneous excitation (*16*). Varying the atomic density by changing the spin-polarized atom number in a fixed lattice environment allows us to determine this density shift precisely, using the high measurement stability of the optical comparison. This shift scales with the atomic excitation fraction and depends on the nuclear spin state. By controlling the relevant system parameters, we are able to measure and control this shift of $8.9(8) \times 10^{-16}$ (see Fig. 3B, with spin polarization to ±9/2, $\rho_0 = 1 \times 10^{11}$ cm^{-3}). We have also observed an excitation fraction for which the density shift is consistent with zero.

Table 1 gives a summary of our investigation of the Sr systematic clock shifts. The probe laser ac Stark shift, line pulling, and servo error are described in (*16*). The overall fractional systematic uncertainty is 1.5×10^{-16}, the smallest uncertainty reported for any neutral atom standard to date and represents an improvement by a factor of 6 over our previous result (*9*). This uncertainty evaluation has enabled an improved absolute frequency measurement of the Sr clock transition (*31*). The evaluation of the Sr clock is now limited by knowledge of Stark shifts of atomic energy levels induced by the room temperature blackbody radiation (BBR) (*32*), a critical issue for developing standards. The highest

Table 1. Systematic frequency corrections and their associated uncertainties for the $^1S_0$-$^3P_0$ clock transition, in units of 10^{-16} fractional frequency.

Contributor	Correction (10^{-16})	Uncertainty (10^{-16})
Lattice Stark (scalar/tensor)	−6.5	0.5
Hyperpolarizability (lattice)	−0.2	0.2
BBR Stark	52.1	1.0
ac Stark (probe)	0.2	0.1
First-order Zeeman	0.2	0.2
Second-order Zeeman	0.2	0.02
Density	8.9	0.8
Line pulling	0	0.2
Servo error	0	0.5
Second-order Doppler	0	<<0.01
Systematic total	54.9	1.5

accuracy calculation of the BBR shift considers both bound- and continuum-state contributions, dynamical corrections to the static polarizability, and higher-order multipole contributions (*33*). At room temperature, the uncertainty in the BBR shift originating from uncertainty in the polarizability (1%) is 7×10^{-17}. Further uncertainty in the BBR shift originates from lack of control and homogeneity of the blackbody environment (at room temperature, T). By monitoring many positions on the Sr vacuum chamber, we determine the blackbody environment to $\Delta T = 1$ K (root mean square, contributions from the thermal Sr oven are negligibly small), leading to a shift uncertainty of 7.5×10^{-17}. Combining the two effects yields a 1×10^{-16} total BBR uncertainty.

To further improve the Sr accuracy, the differential static polarizability of the clock states must be known to better than 1% (with the dynamical correction contributing <5% to the total shift). This can be measured directly by enclosing the atoms in a well-characterized blackbody environment and recording the clock shift as this temperature is systematically varied (this simultaneously decreases uncertainty in the BBR environment). The technical challenge lies in the control of temperature homogeneity over various functional areas of the vacuum chamber while accommodating sufficient optical access for a variety of atomic manipulations. One possible solution is to cool and trap atoms in a standard chamber and then transport them in a moving lattice (*34*) to a secondary chamber, where an ideal, well-defined blackbody environment is established (*16*). Such an approach avoids the complexity of cryogenic operation and can be generalized to other lattice clock species. These improvements can potentially improve the BBR-related uncertainty to far below 10^{-16}.

References and Notes

1. T. P. Heavner, S. R. Jefferts, E. A. Donley, J. H. Shirley, T. E. Parker, *Metrologia* **42**, 411 (2005).
2. S. Bize *et al.*, *J. Phys. B* **38**, S449 (2005).
3. L. Hollberg *et al.*, *J. Phys. B* **38**, S469 (2005).
4. M. M. Boyd *et al.*, *Science* **314**, 1430 (2006).
5. W. H. Oskay *et al.*, *Phys. Rev. Lett.* **97**, 020801 (2006).
6. H. S. Margolis *et al.*, *Science* **306**, 1355 (2004).
7. T. Schneider, E. Peik, C. Tamm, *Phys. Rev. Lett.* **94**, 230801 (2005).
8. D. Leibfried, R. Blatt, C. Monroe, D. Wineland, *Rev. Mod. Phys.* **75**, 281 (2003).
9. M. M. Boyd *et al.*, *Phys. Rev. Lett.* **98**, 083002 (2007).
10. Z. W. Barber *et al.*, *Phys. Rev. Lett.* **96**, 083002 (2006).
11. M. Takamoto *et al.*, *J. Phys. Soc. Jpn.* **75**, 104302 (2006).
12. X. Baillard *et al.*, *Eur. Phys. J. D*, published online 7 December 2007; 10.1140/epjd/e2007-00330-3.
13. D. Jaksch, P. Zoller, *Ann. Phys.* **315**, 52 (2005).
14. T. M. Fortier *et al.*, *Phys. Rev. Lett.* **98**, 070801 (2007).
15. S. Schiller *et al.*, *Nuc. Phys. B Proc. Suppl.* **166**, 300 (2007).
16. Additional details are available as supporting material on *Science* Online.
17. S. M. Foreman *et al.*, *Phys. Rev. Lett.* **99**, 153601 (2007).
18. T. Fortier, A. Bartels, S. A. Diddams, *Opt. Lett.* **31**, 1011 (2006).
19. C. W. Oates *et al.*, *IEEE Inter. Freq. Control Symposium and Exposition*, 74 (June 2006).
20. W. M. Itano *et al.*, *Phys. Rev. A* **47**, 3554 (1993).
21. G. Santarelli *et al.*, *IEEE Trans. Ultrason. Ferroelec. Freq. Cont.* **45**, 887 (1998).
22. A. D. Ludlow *et al.*, *Opt. Lett.* **32**, 641 (2007).
23. H. Katori, M. Takamoto, V. G. Pal'chikov, V. D. Ovsiannikov, *Phys. Rev. Lett.* **91**, 173005 (2003).
24. A. D. Ludlow *et al.*, *Phys. Rev. Lett.* **96**, 033003 (2006).
25. A. Brusch, R. Le Targat, X. Baillard, M. Fouche, P. Lemonde, *Phys. Rev. Lett.* **96**, 103003 (2006).
26. M. M. Boyd *et al.*, *Phys. Rev. A* **76**, 022510 (2007).
27. D. E. Chang, J. Ye, M. D. Lukin, *Phys. Rev. A* **69**, 023810 (2004).
28. M. W. Zwierlein, Z. Hadzibabic, S. Gupta, W. Ketterle, *Phys. Rev. Lett.* **91**, 250404 (2003).
29. R. Santra, K. V. Christ, C. H. Greene, *Phys. Rev. A* **69**, 042510 (2004).
30. P. G. Mickelson *et al.*, *Phys. Rev. Lett.* **95**, 223002 (2005).
31. The absolute frequency measurement made over a 48-hour period determined the clock frequency to within a total uncertainty of 8.6×10^{-16}, limited by uncertainties in the NIST maser and F1 Cs fountain operation. The final result agrees with our previous measurement (*9*). For more details, see (*35*).
32. L. Hollberg, J. L. Hall, *Phys. Rev. Lett.* **53**, 230 (1984).
33. S. G. Porsev, A. Derevianko, *Phys. Rev. A* **74**, 020502R (2006).
34. S. Schmid, G. Thalhammer, K. Winkler, F. Lang, J. H. Denschlag, *N. J. Phys.* **8**, 159 (2006).
35. S. Blatt *et al.*, *Phys. Rev. Lett.*, in press; http://arXiv.org/abs/0801.1874.

36. We thank X. Huang for technical help in operating the Sr clock. This research is supported by the Office of Naval Research, National Institute of Standards and Technology, National Science Foundation, and Defense Advanced Research Projects Agency. A.D.L. acknowledges support from NSF-IGERT through the OSEP program at CU. G.K.C. acknowledges support from the National Research Council.

Supporting Online Material

www.sciencemag.org/cgi/content/full/1153341/DC1
SOM Text
Fig. S1
References

26 November 2007; accepted 23 January 2008
Published online 14 February 2008;
10.1126/science.1153341
Include this information when citing this paper.

Frequency Ratio of Al^+ and Hg^+ Single-Ion Optical Clocks; Metrology at the 17th Decimal Place

T. Rosenband,* D. B. Hume, P. O. Schmidt,† C. W. Chou, A. Brusch, L. Lorini,‡ W. H. Oskay,§ R. E. Drullinger, T. M. Fortier, J. E. Stalnaker,‖ S. A. Diddams, W. C. Swann, N. R. Newbury, W. M. Itano, D. J. Wineland, J. C. Bergquist

Time has always had a special status in physics because of its fundamental role in specifying the regularities of nature and because of the extraordinary precision with which it can be measured. This precision enables tests of fundamental physics and cosmology, as well as practical applications such as satellite navigation. Recently, a regime of operation for atomic clocks based on optical transitions has become possible, promising even higher performance. We report the frequency ratio of two optical atomic clocks with a fractional uncertainty of 5.2×10^{-17}. The ratio of aluminum and mercury single-ion optical clock frequencies ν_{Al^+}/ν_{Hg^+} is 1.052871833148990438(55), where the uncertainty comprises a statistical measurement uncertainty of 4.3×10^{-17}, and systematic uncertainties of 1.9×10^{-17} and 2.3×10^{-17} in the mercury and aluminum frequency standards, respectively. Repeated measurements during the past year yield a preliminary constraint on the temporal variation of the fine-structure constant α of $\dot{\alpha}/\alpha = (-1.6 \pm 2.3) \times 10^{-17}$/year.

Time is the physical coordinate over which humans have the least control, and yet it is the most accurately realized fundamental unit. Although any physical system that evolves predictably can serve as a time base, isolated atoms have long been recognized as near-ideal references for laboratory clocks, due to the abundance of identical copies, as well as their